A New Wideband Electromagnetic Vibration Energy Harvester with Chaotic Oscillation

Takahiro Sato[1], **Hajime Igarashi**
Graduate School of information science and technology, Hokkaido University,
Kita 14, Nishi 9, Kita-ku, Sapporo, 060-0814, JAPAN.

E-mail: tsato@em-si.eng.hokudai.ac.jp

Abstract. This paper presents a new electromagnetic vibration energy harvester (VEH) which harvests the electric power in wide frequency range. The present VEH contains the ferrite core embedded in the axis hole of the coil bobbin which generates the magnetic force acting on the oscillator. The performance of the present VEH is estimated using the coupled analysis method for VEH in which motion, Ampere, and circuit equations are alternatively solved until convergence. Using the coupled analysis method, the output power characteristic in the present VEH against input frequency is analyzed. It is shown from the analysis results that the present VEH has chaotic oscillation and wide frequency range for power generation. Moreover, the condition that the present VEH has nonlinear oscillation is discussed.

1. Introduction

The electromagnetic vibration energy harvesters (VEHs) [1]-[4] have received much attention as new small power source for wireless sensor network systems. The sensor nodes with VEHs can harvest the electric power from their environment. Using VEHs, it is possible to realize wireless sensor systems which are free from the battery replacements. For the developments of practical VEH systems, the output power in VEHs must be improved. In addition, the VEHs are required to harvest power in wide frequency range. However, when the VEH has linear oscillation, output can only be obtained near to the resonant frequency. It has been indicated that the nonlinearity in the VEHs can expand the bandwidth [5], [6]. For this reason, the nonlinear VEHs have been developed recently [7], [8]. Because the oscillators in the VEHs with nonlinearity have complicated motion, the conventional spring-damper theory [9] is not applicable to estimate their performance. This is one of the reasons that it is difficult to design the nonlinear VEHs.

In this paper, we present a nonlinear VEH which has wide operation range. The present VEH contains ferrite core embedded in the axis hole of the coil bobbin which generates the magnetic force acting on the oscillator. Because of the magnetic force, the oscillator in the present VEH has complicated motion. To estimate the performance of the present VEH, the coupled analysis method of VEH [10] is employed in which motion, Ampere, and circuit equations are alternatively solved until convergence. It is numerically shown from the analysis results that the present VEH has chaotic oscillation. It is also shown that the preset VEH has wide frequency range for power generation. Moreover, the reason that the present VEH has nonlinear oscillation is discussed.

[1] Corresponding author: Takahiro Sato

2. Coupled analysis method for VEH [10]

The performance of the conventional linear VEH can be estimated from the spring-damper model [8], while, that of the nonlinear VEHs cannot be estimated using it. To estimate the nonlinear VEHs, we have presented the coupled analysis method for VEH, which numerically solves the following equations:

$$m(\ddot{p}-\ddot{q})+c_{\mathrm{m}}(\dot{p}-\dot{q})+k_{\mathrm{m}}(p-q)-F(\boldsymbol{A})=0, \tag{1}$$

$$\nabla\times\nu(\nabla\times\boldsymbol{A})=\boldsymbol{J}+\nu_0\nabla\times\boldsymbol{M}, \tag{2}$$

$$\mathrm{Z}(\boldsymbol{i})\boldsymbol{i}=\boldsymbol{V}(\boldsymbol{A}), \tag{3}$$

where m is mass of objects on the tip of the oscillator, c_{m} and k_{m} are effective damping and stiffness coefficients of the oscillator, p and q are the oscillator and base displacements, respectively. In addition, $\boldsymbol{A}$, $\boldsymbol{M}$, ν and ν_0 are vector potential, magnetization vector, reluctivity of magnetic material and vacuum, respectively. Moreover, $F(\boldsymbol{A})$ and $\boldsymbol{J}$ are the magnetic force acting on the oscillator and the current density in the coil, respectively, $\mathrm{Z}(\boldsymbol{i})$ is the impedance matrix for a circuit, and $\boldsymbol{V}(\boldsymbol{A})$ is the voltage vector corresponding to the electromotive force (EMF) induced in the coils which is calculated as follows:

$$\left(\boldsymbol{V}(\boldsymbol{A})\right)_i=\int_{V_i^C}\frac{\mathrm{D}\boldsymbol{A}}{\mathrm{D}t}\cdot\boldsymbol{l}_i\mathrm{d}V, \tag{4}$$

where D/Dt is the Lagrange derivative to consider EMF due to the coil movement, and V_i^C, $\boldsymbol{l}_i$ are the volume of the coil and the tangential vector of the current in the coil for circuit loop i, respectively. Note that, if no coil is included the loop i, $(\boldsymbol{V}(\boldsymbol{A}))_i$ is zero.

In the coupled analysis, the governing equations are discretized with respect to time and alternatively solved until convergence at each time step. This iteration is here called sub-cycle. When the all solutions converge in the sub-cycle, that is,

$$\left|p_n^k-p_n^{k-1}\right|<\varepsilon_p,\left\|\boldsymbol{A}_n^k-\boldsymbol{A}_n^{k-1}\right\|<\varepsilon_A,\left\|\boldsymbol{i}_n^k-\boldsymbol{i}_n^{k-1}\right\|<\varepsilon_I, \tag{5}$$

then the time is incremented, and new sub-cycle starts, where n and k is the iteration number of time and sub-cycle, respectively. Here, (1) and (3) are solved using the Runge-kutta and Newton-Raphon methods, respectively. In addition, (2) is solved by the finite element method for electromagnetic field in which, to easily treat the moving objects, the nonconforming technique is employed. The flow of the coupled analysis is shown in figure 1.

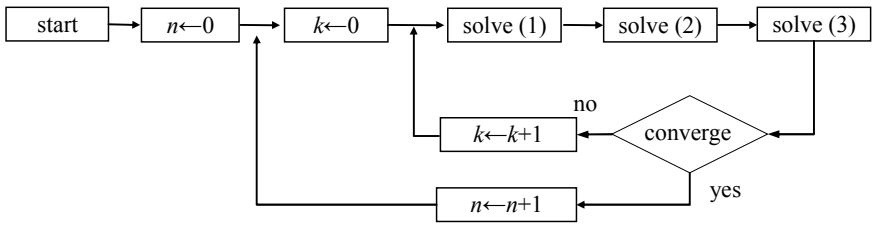

Figure 1. Flowchart of coupled analysis method.

3. Chaotic vibration energy harvester

We consider here the nonlinear VEH shown in figure 2 which contains the ferrite core embedded in the axis hole of the coil bobbin. The ferrite core forms nearly closed flux path with the magnets to increase the flux across the coil. In addition, the magnetic force acting on the magnets is generated, which makes the cantilever motion complicated and gives rise to nonlinear oscillation in the present VEH. When the oscillation becomes chaotic due to the nonlinearity, the frequency range in this system would become wider.

In this work, the performance of the present VEH is analyzed using the coupled analysis method. The mechanical parameters of the cantilever are summarized in Table 1. The full-wave rectifier and the storage capacitor whose capacitance is 1mF are connected to the present VEH as shown in figure 3, where threshold voltage of diodes and winding resistance are set to 0.2V and 100Ω, respectively. The output characteristic against the input frequency, f, is analyzed where the input amplitude is set to 0.1mm.

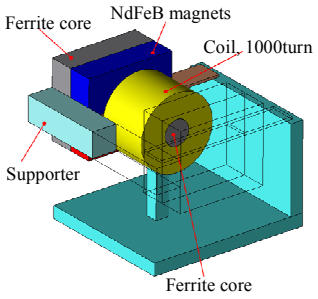

Figure 2(a). Overview of present VEH.

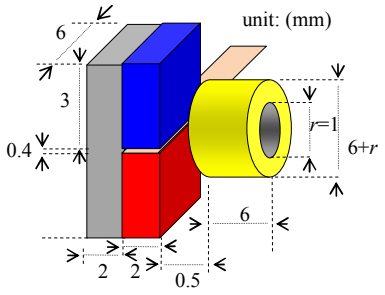

Figure 2(b). Sizes specification.

Table 1. Mechanical parameters in present VEH.

k_m	c_m	m
600 N/m	0.05 Ns/m	3.5 g

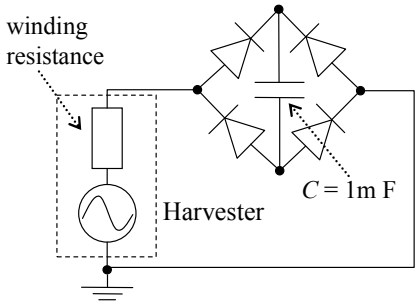

Figure 3. Full-wave rectifier circuit.

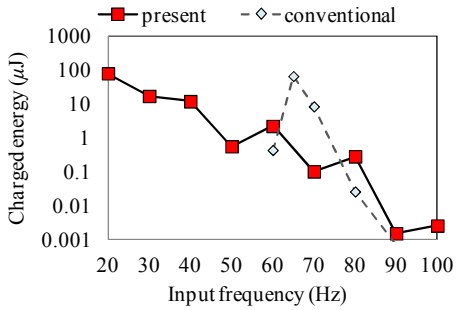

Figure 4. Charged energy against frequency.

The electric energy charged in the capacitor over 20 input cycles is shown in figure 4, in which the energy obtained by the VEH without the ferrite core (conventional VEH) is also shown to clarify the effect of the introduction of the ferrite core. Note that the energy under 0.001μJ is not plotted. It can be seen from figure 4 that we can have wider frequency range for power generation in comparison with the conventional VEH. The trajectories in the z-v plane are shown in figure 5, where $z=p-q$ and $v=\dot{p}-\dot{q}$ represent relative displacement and velocity, respectively. The transitions of z and induced voltage, V, are shown in figure 6. We can see that the cantilever oscillation has higher harmonics especially when f is 50Hz and 80Hz. To analyze the complicity in the oscillation, the Lyapunov exponent, λ, is computed using the Rosenstein's method [11], where positive value corresponds to chaotic motion. The Lyapunov exponents for all frequency are shown in figure 7, from which we can see that the cantilever oscillations are chaotic. From these results, it can be said that the chaotic oscillation can expand the operation frequency range for power generation.

To reveal the condition that the present VEH has chaotic motion, the distribution of λ in r-f plane is plotted in figure 8, where r denotes the diameter of the ferrite core embedded in the coil bobbin. In figure 8, the VEH has no oscillation when λ is 0. We can see that λ is positive in wide frequency range

when r is small, while λ is negative at high frequencies when r is large. This result suggests that there is a lower limit for r to have chaotic motion in the VEH. Furthermore, linear oscillation is observed when r is large.

Here, we discuss the reason why the present VEH has chaotic and linear oscillations when r is small and large, respectively. Figure 9 shows the magnetic force acting on the magnets when r is 1mm and 4mm, respectively, in addition to the spring force. We can see from figure 9 that the magnetic force is has the same direction to the spring force when r=4mm, while its direction is reverse when r=1mm. This is because the flux path completely changes depending on r as shown in figure 10. The total force of magnetic and spring force is shown in figure 11 from which it can be seen that the total force when r=1mm is clearly nonlinear with respect to the relative displacement. As a result, the nonlinearity is given rise to the present VEH. On the other hand, when r=4mm, the magnetic force enhances spring force, and the initial total force is linear with respect to the relative displacement. Thus, the VEH has linear oscillation at high frequencies when r is large. The reason why the VEH has no oscillation at low frequencies is that the resonant frequency gets larger in comparison with the original one of the VEH, because the effective spring constant becomes larger due to the magnetic force.

From these discussions, it can be said that one can design the nonlinear VEH by creating the flux path using the magnetic material to generate the magnetic force whose direction is opposite to the spring force.

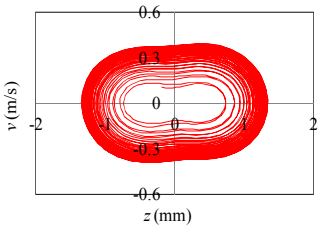

Figure 5(a). Trajectory for 20Hz.

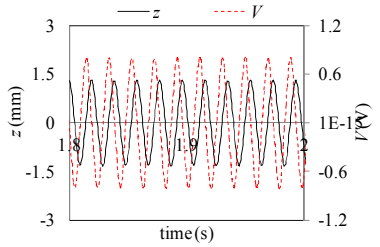

Figure 6(a). Transitions for 20Hz.

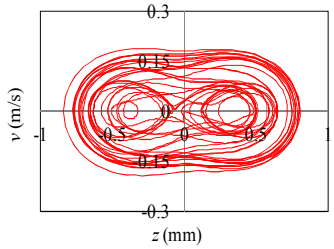

Figure 5(b). Trajectory for 50Hz.

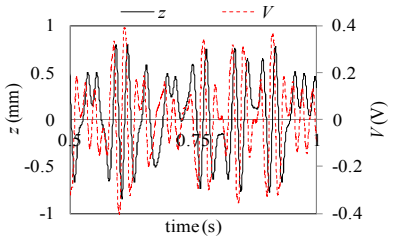

Figure 6(b). Transitions for 50Hz.

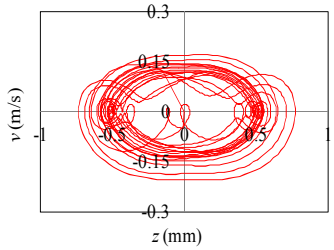

Figure 5(c). Trajectory for 80Hz.

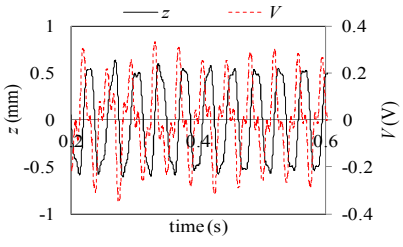

Figure 6(c). Transitions for 80Hz.

4. Conclusion

The new nonlinear VEH which contains ferrite core embedded in the axis hole of the coil bobbin has been presented. The performance of the present VEH is analyzed using the coupled analysis method. It is shown that the present VEH has chaotic oscillation. It is also found from the simulation that the

present VEH has wide frequency range for power generation in comparison with conventional linear VEH. Moreover, the condition that the present VEH has chaotic oscillation is shown based on the distribution of the Lyapunov exponent in *z-f* plane. The numerical result has suggested that *r* must be smaller than a curtain threshold to have the chaotic motion.

For the future works, the analysis results of the present VEH will be compared with measurement data.

5. Acknowledgment

This study was supported by research grants from Japan Power Academy and a Grant-in-Aid for Scientific Research (24310117).

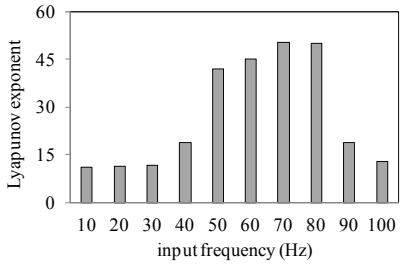

Figure 7. Lyapunov exponents for *z*.

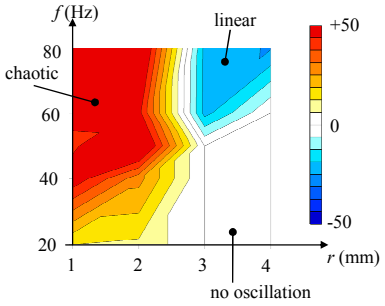

Figure 8. Distribution of Lyapunov exponents.

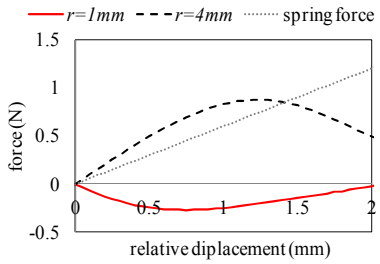

Figure 9. Magnetic and spring force.

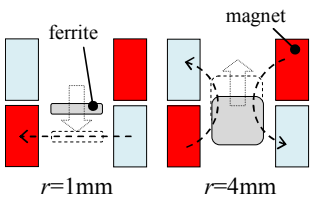

Figure 10. Flux path in VEH.

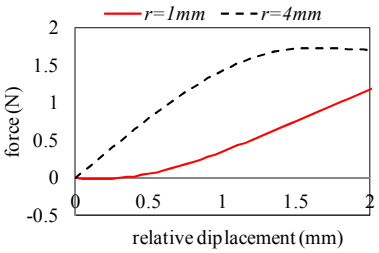

Figure 11. Total force.

6. References

[1] S. P. Beeby, R. N. Torah, M. J. Tudor, P. Glynne-Jones, T. O'Donnell, C. R. Saha and S. Roy, *Micromech. Microeng* 2007, vol. 17, pp 1257-1265.
[2] Dibin Zhu, Stephen Roberts, Thomas Mouille, Michael J Tudor, and Stephen P Beeby, *Smart Mater. Struct*., 2012, vol. 21, pp. 1-14.
[3] Yingjun Sang, Xueliang Huang, Hexiang Liu, and Ping Jin, *IEEE Trans. Magn.*, 2012, vol. 48, No. 11, pp.4495-4498.
[4] Yang Zhu and Jean W. Zu, *IEEE Trans. Magn*., 2012, vol 48, No. 11, pp. 3344-3347.
[5] Lars Geir Whist Tvedt, Duy Son Nguyen, and Einar Halvorsen, *Journal of Microelectromechanical systems*, 2010, vol. 19, No. 2, pp. 305-316.
[6] M. Ferrari, V. Ferrari, M. Guizzetti, B. Andò, S. Baglio, C. Trigona, *Sensors and actuators A*, 2010, Vol. 162, pp. 425-431.
[7] A. Erturk, D.J.Inman, *Journal of Sound and Vibration*, 2011, vol. 330, pp 2339–2353.
[8] Louis Van Blarigan, Per Danzl, Jeff Moehlis, *Appl. Phys. Lett.*, 2012, 100, 253904.
[9] N.G. Stephen, *Journal of Sound and Vibration*, 2006, vol. 293, pp. 409–425.
[10] T. Sato, K. Watanabe, H. Igarashi, *IEEE Trans. Magn.*, 2014 (to be published)
[11] Michael T. Rosenstein, James J. Collins, Carlo J. De Luca, 1993, *Physica D*, vol 65, pp. 117-134.